



REGULAR ARTICLE

Mathematical Modeling of Permissible Thermoelastic Stress Distribution in Optical Elements of Electrical Power Systems

I.V. Yatsenko^{1,*} , V.S. Antonyuk², V.A. Vashchenko¹, V.I. Gordienko¹, V.P. Maslov³, T.I. Butenko¹

¹ Cherkasy State Technological University, 18006 Cherkassy, Ukraine

² National Technical University of Ukraine "Kyiv Polytechnic Institute named after Igor Sikorsky", 03056 Kyiv, Ukraine

³ V.E. Lashkaryov Institute of Semiconductor Physics NAS of Ukraine, 02000 Kyiv, Ukraine

(Received 02 December 2025; revised manuscript received 15 February 2026; published online 25 February 2026)

Mathematical models have been developed to describe the thermal influence of a strip electron beam (SEB) on optical elements, taking into account the results of beam sensing, the geometric shape and dimensions of the elements, as well as the temperature dependence of the thermophysical properties of the optical material (volumetric heat capacity and thermal conductivity coefficient), which makes it possible to more accurately calculate the temperature and thermoelastic stress distributions across the thickness of the optical element in the regions of maximum external SEB influence. The proposed models make it possible to more accurately calculate the effect of controllable parameters of the electron-beam installation (beam current, accelerating voltage, distance to the treated surface, and SEB scanning speed) on the distribution of thermoelastic stresses across the thickness of the elements and to determine the permissible ranges of their variation, the exceedance of which leads to the destruction of the elements and failure of electrical power system components based on them. This makes it possible to increase the efficiency of final surface treatment of optical components made of optical ceramics using SEB technology, with the aim of improving the mechanical strength of their surface layers, which ultimately enhances the reliability, safety, and stable operation of electrical power system components under extreme electrical and thermal loads.

Keywords: Mathematical models, Electrical power systems, Electron-beam technology, Optical ceramic, Methods of heat conduction and thermoelasticity theory.

DOI: [10.21272/jnep.18\(1\).01004](https://doi.org/10.21272/jnep.18(1).01004)

PACS number: 42.79.Bh

1. INTRODUCTION

During operation, components of electrical power systems (such as optical protective windows in power equipment, sensors, thermal imaging devices, and heat-resistant optical instruments) [1-3] are subjected, on certain surface areas, to extreme electrical and thermal effects (local maximum external heating, spark discharges, high-temperature fields, etc.), which lead to the formation of cracks, chipping, and detrimental structural changes in the surface layers. These processes result in a significant deterioration of the components performance and, ultimately, their failure. Therefore, in order to improve the properties of the surface layers – specifically, to increase microhardness and to form thermally strengthened layers without impairing the infrared transmission coefficient of optical ceramics such as KO₂, KO₄, KO₁₂, and others – these surface areas are additionally treated with a strip electron beam (SEB) [1, 4-6].

However, when using a strip electron beam (SEB) for surface treatment of the above-mentioned components, critical local overheating may occur in their surface layers, causing the presence of induced relaxation thermoelastic stresses that exceed the allowable limits for the given material. Therefore, at the stage of developing

technological processes for surface treatment of products made of optical materials, it is necessary to be able to predict the distribution of thermal stresses in these components depending on the controllable SEB parameters and to determine the permissible modes of their surface thermal strengthening. At present, only the temperature fields in treated optical elements of various geometric shapes and dimensions (plane-parallel plates, cylindrical rods, disks, spherical and hemispherical elements, rectangular elements of various thicknesses, etc.) under the influence of a moving SEB [1, 6-9] have been sufficiently studied. As for investigations of thermoelastic stress distributions along the surface of optical elements and across their thickness, they remain rather limited. Data on determining the critical ranges of variation of thermoelastic stresses in the SEB-affected zones are completely absent.

Therefore, the purpose of this work is to apply mathematical modeling methods of the thermal influence of a moving SEB on optical elements of electrical power system components in order to determine the permissible ranges of variation of its parameters, the exceedance of which leads to the degradation of the technical and operational characteristics of the components, up to their destruction.

* Correspondence e-mail: i.yatsenko@chdtu.edu.ua



2. THE RESULTS OF THE RESEARCH AND THEIR ANALYSIS

Rectangular optical elements of various thicknesses, which are widely used in electrical power system components, are considered as the objects of the study [2, 5, 6].

Mathematical models of temperature fields and thermoelastic stresses in the zones of maximum thermal influence of the SEB on optical elements.

For the considered rectangular element, the following conditions are assumed: the depth of the thermal influence zone $\delta \sim H$ and $\delta > B$, i.e. $\frac{\partial T}{\partial y} = 0$ (a

two-dimensional temperature field $T(x, z, t)$ is considered); In this case, the medium along the Oz axis is treated as bounded, taking into account heat exchange on its lower side (Fig. 1). The treated element is placed on a thermally insulating substrate, so that radiative and convective heat losses from its lower side can be neglected in the first approximation. In the absence of radiative and convective heat losses from the element's surface, heat exchange at its lower side ($z = H$) corresponds to adiabatic conditions of the thermal process.

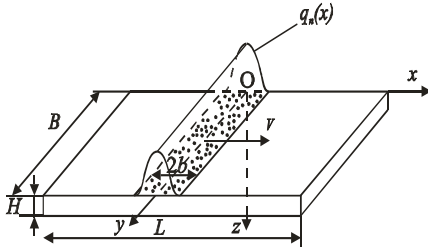


Fig. 1 – Schema of the process of heating a rectangular element with a moving SEB: $2b$ – thickness of the moving electron beam; B , H , L – width, thickness and length of the element, m; V – speed of movement of SEB, m/s; $Oxyz$ – rectangular coordinate system, which is related to the SEB

As a result of the conducted experimental investigations on SEB profiling [1, 6, 10, 11], it was established that the SEB exhibits a normal distribution of energy flux density (or thermal influence density) $q_n(x)$ across the thickness of the electron beam (for $I_b = 50 \dots 300$ mA; $V_y = 4 \dots 8$ kV; $l = 60 \dots 80$ mm):

$$q_n(x) = \begin{cases} \frac{P_0(I_b, V_y) \times \sqrt{k_0(I_b, l)} \times e^{-k_0(I_b, l) \times x^2}}{B \times \sqrt{\pi} \times \text{erf}\left[b(I_b, l) \times \sqrt{k_0(I_b, l)}\right]}, & |x| < b \\ 0, & |x| > b, \end{cases} \quad (1)$$

$$\text{where } P_0 = I_b \cdot V_y; \quad (2)$$

$$k_0(I_b, l) = 9,367 \cdot 10^7 - 7,859 \cdot 10^5 \cdot l - (5,1 \cdot 10^4 - 1,3 \cdot 10^3 \cdot l) \cdot I_b; \quad (3)$$

$$b(I_b, l) = \frac{1,73}{\sqrt{k_0(I_b, l)}}. \quad (4)$$

Here, P_0 is the SEB power, W ; k_0 – is the concentration coefficient of the electron beam, m^{-2} . Under the above assumptions, the equations of the

mathematical model for the heating process of the considered element (in the moving coordinate system associated with the SEB) take the following form:

$$C_V(T) \cdot \frac{\partial T}{\partial t} = \frac{\partial}{\partial x} \left(\lambda(T) \cdot \frac{\partial T}{\partial x} \right) + \frac{\partial}{\partial z} \left(\lambda(T) \cdot \frac{\partial T}{\partial z} \right) + C_V(T) \cdot V \cdot \frac{\partial T}{\partial x},$$

$$t > 0, \quad -\infty < x < +\infty, \quad 0 < z < H, \quad (5)$$

$$T|_{t=0} = T_0, \quad (6)$$

$$-\lambda(T) \cdot \frac{\partial T}{\partial z} \Big|_{z=0} = q_n(x), \quad (7)$$

$$\lambda(T) \cdot \frac{\partial T}{\partial z} \Big|_{z=H} = 0, \quad (8)$$

$$T \rightarrow T_0, \quad \left(\frac{\partial T}{\partial x} \right) \rightarrow 0 \text{ at } x \rightarrow \pm\infty, \quad (9)$$

where $C_V(T)$ and $\lambda(T)$ are the volumetric heat capacity ($J/m^3 \cdot K$) and thermal conductivity ($W/(m \cdot K)$) of the element material, respectively.

Equations (5) – (9) take into account the empirical dependences $C_V(T) = C_{V0} \cdot T^\nu$, $\lambda(T) = \lambda_0 \cdot T^\nu$ [1, 6, 12].

By applying the well-known methods of linearizing equations (5)-(8) [12], as well as Fourier integral transform methods (first with respect to the x -coordinate and then with respect to the z -coordinate, and taking into account (1)-(4) and the dependencies of $C_V(T)$ and $\lambda(T)$ we obtain the following expression for $T(x, z, t)$:

$$T(x, z, t) = \left\{ T_0^{\nu+1} + \frac{V_{xx} \cdot V^2 \cdot x t}{2a_0^2 \cdot 4a_0^2} + \frac{(\nu+1) \times a_0 \times I_b \times V_y \times \sqrt{k_0(I_b, l)} \times e^{-\frac{V_{xx} \cdot V^2 \cdot x t}{2a_0^2 \cdot 4a_0^2}}}{4\pi \times B \times \lambda_0 \times \text{erf}\left[b(I_b, l) \times \sqrt{k_0(I_b, l)}\right]} \right. \\ \left. \frac{V^2 \cdot \tau \cdot 4a_0^2 \cdot k_0(I_b, l) \cdot x^2 - V \cdot [2x + V(t-\tau)]}{4a_0^2 \cdot 4a_0^2 \cdot [1 + 4a_0^2 \cdot k_0(I_b, l) \cdot (t-\tau)]} \right. \\ \left. \int_0^t \frac{e^{-\frac{V^2 \cdot \tau \cdot 4a_0^2 \cdot k_0(I_b, l) \cdot (t-\tau) - V \cdot [2x + V(t-\tau)]}{4a_0^2 \cdot 4a_0^2 \cdot [1 + 4a_0^2 \cdot k_0(I_b, l) \cdot (t-\tau)]}}}{\sqrt{1 + 4a_0^2 \cdot k_0(I_b, l) \cdot (t-\tau)} \cdot \sqrt{t-\tau}} \cdot \left[\frac{1}{2} + \sum_{n=0}^N \cos\left(\frac{\pi \cdot n \cdot z}{H}\right) \cdot e^{-\left(\frac{\pi \cdot n \cdot a_0}{H}\right)^2 \cdot (t-\tau)} \right] \right. \\ \left. \cdot \text{erf}\left[\sqrt{\frac{1 + 4a_0^2 \cdot k_0(I_b, l) \cdot (t-\tau)}{4a_0^2 \cdot (t-\tau)}} \cdot \left(b(I_b, l) + \frac{x + V \cdot (t-\tau)}{1 + 4a_0^2 \cdot k_0(I_b, l) \cdot (t-\tau)} \right) \right] + \right. \\ \left. + \text{erf}\left[\sqrt{\frac{1 + 4a_0^2 \cdot k_0(I_b, l) \cdot (t-\tau)}{4a_0^2 \cdot (t-\tau)}} \cdot \left(b(I_b, l) - \frac{x + V \cdot (t-\tau)}{1 + 4a_0^2 \cdot k_0(I_b, l) \cdot (t-\tau)} \right) \right] \right] \frac{1}{V^{\nu+1}} \quad (10)$$

The thermoelastic stresses arising in the surface layers of the considered rectangular element are evaluated at their maximum (in the areas where the

heat flux $q_n(x)$ and temperature $T(x, z, t)$ reach their highest values: $q_{n\max} = q_n(0)$; $T_{\max}(z, t) = T(0, z, t)$, i.e., at the center of the SEB thermal action (Fig. 2). This approach allows for assessing, across the entire surface of the element, the permissible ranges of variation of the controllable SEB parameters – electron beam current I_b , mA; accelerating voltage V_y , kV; distance from the treated surface l , m; beam scanning speed V , m/s; and exposure time t , s), in which there is no surface destruction during the entire processing process.

In the considered case, the occurrence of thermoelastic stresses is associated with the temperature gradient across the thickness of the element (along the Oz axis), and their magnitude $\sigma_{\max}(z, t)$, is expressed as follows [1, 6, 12-14]:

$$\sigma_{\max}(z, t) = \frac{\alpha_v \cdot E}{1 - \nu} \cdot \left[-T_{\max}(z, t) + \frac{2}{H^2} \cdot (2H - 3z) \int_0^H T_{\max}(z, t) dz - \frac{6}{H^3} \cdot (H - 2z) \cdot \int_0^H T_{\max}(z, t) z dz \right]. \quad (11)$$

The temperature profile is found from expression (10) at $x = 0$:

$$T_{\max}(z, t) = \begin{cases} T_0^{\nu+1} + \frac{(\nu+1) \cdot a_0 \cdot I_L \cdot V_y \cdot \sqrt{k_0(I_b, l)} \cdot e^{-\frac{V^2 \cdot t}{4a_0^2}}}{4\pi \cdot B \cdot \lambda_0 \cdot \operatorname{erf}(b(I_b, l) \cdot \sqrt{k_0(I_b, l)})} \\ \frac{V^2 \cdot \tau + V^2 \cdot (t - \tau)}{4a_0^2 \cdot 4a_0^2 \cdot [1 + 4a_0^2 \cdot k_0(I_b, l) \cdot (t - \tau)]} \\ \cdot \int_0^t \frac{e^{-\frac{V^2 \cdot \tau}{4a_0^2}}}{\sqrt{1 + 4a_0^2 \cdot k_0(I_b, l) \cdot (t - \tau)} \cdot \sqrt{t - \tau}} \\ \cdot \left[\frac{1}{2} + \sum_{n=0}^N \cos\left(\frac{\pi \cdot n \cdot z}{H}\right) \cdot e^{-\left(\frac{\pi \cdot n \cdot a_0}{H}\right)^2 \cdot (t - \tau)} \right] \\ \cdot \operatorname{erf}\left(\sqrt{\frac{1 + 4a_0^2 \cdot k_0(I_b, l) \cdot (t - \tau)}{4a_0^2 \cdot (t - \tau)}} \cdot \left(b(I_b, l) + \frac{V \cdot (t - \tau)}{1 + 4a_0^2 \cdot k_0(I_b, l) \cdot (t - \tau)}\right)\right) + \\ + \operatorname{erf}\left(\sqrt{\frac{1 + 4a_0^2 \cdot k_0(I_b, l) \cdot (t - \tau)}{4a_0^2 \cdot (t - \tau)}} \cdot \left(b(I_b, l) - \frac{V \cdot (t - \tau)}{1 + 4a_0^2 \cdot k_0(I_b, l) \cdot (t - \tau)}\right)\right) \end{cases} \cdot \frac{1}{\nu+1}. \quad (12)$$

Using the obtained formulas (11) and (12), it is possible to calculate the dependencies of thermoelastic stress magnitudes in the surface layers of rectangular optical ceramic elements on the controllable SEB parameters and to determine the permissible ranges of variation of these parameters that do not lead to the destruction of the optical material.

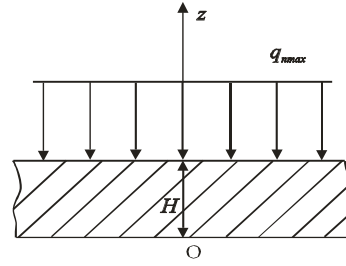


Fig. 2 – Scheme of heating a bar in the area of its surface with maximum thermal influence

Calculations of the influence of SEB parameters on the distributions of thermoelastic stresses in optical elements, selection of permissible surface thermal strengthening modes, and comparison with experimental data.

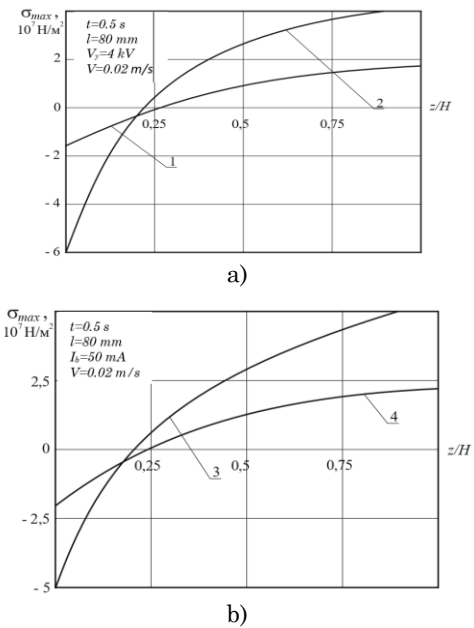


Fig. 3 – Distribution of thermoelastic stresses across the thickness of a rectangular element depending on the SEB parameters ($T_0 = 400$ K; $\alpha_0^2 = 3,3 \cdot 10^{-5}$ m²/s, $\nu = -0,143$; $B = 0,01$ m; $H = 0,04$ m; $L = 0,1$ m; $\lambda_0 = 41,46$ W/m \cdot K $\nu+1$; $\alpha_v(T)$ and $E(T)$): a) – influence of the electron flow current I_b (1 – $I_b = 50$ mA, 2 – $I_b = 100$ mA); b) – the influence of the electron flow velocity V (3 – $V = 0,005$ m/s, 4 – $V = 0,02$ m/s)

To perform the calculations of thermoelastic stresses in the considered rectangular elements (see (11), (12)), standard application software packages were used, along with the necessary thermophysical and physicomaterial properties of the optical material (KO2 ceramics) [3, 7-9]. From the results of the performed calculations (Figs. 3-5), it follows that compressive stresses occur near the upper surface of the rectangular element ($\sigma_{\max} < 0$, $|\sigma_{\max}| = 0,2 \cdot 10^8 \dots 2,3 \cdot 10^8$ N/m²), while tensile stresses occur on the lower surface ($\sigma_{\max} > 0$ ($|\sigma_{\max}| = 1,8 \cdot 10^7 \dots 4,9 \cdot 10^7$ N/m²). The influence of SEB parameters on the magnitude of $|\sigma|$ is as follows: an increase in I_b from 50 mA to 150 mA and an increase in V_y from 4 kV to 8 kV lead to an increase in $|\sigma|$ by

approximately 6-8 times and 3-4 times, respectively, whereas an increase in V from 0.01 m/s to 0.05 m/s and l from 60 mm to 80 mm results in a decrease in $|\sigma_{\max}|$ by approximately 2-3 times and 1.1-1.2 times, respectively.

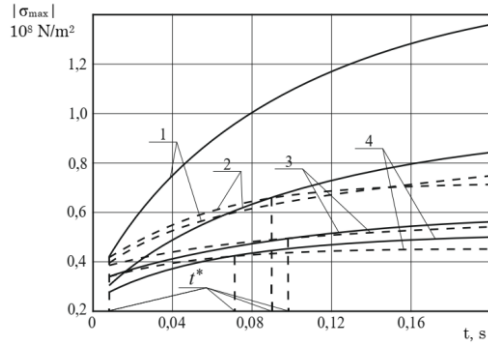
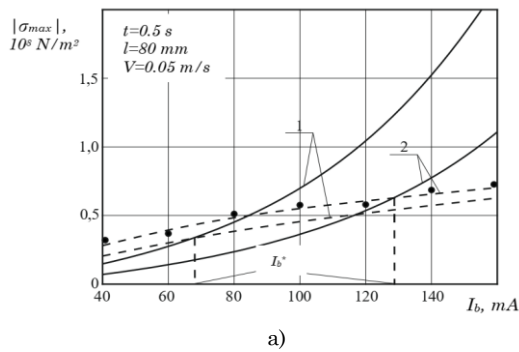
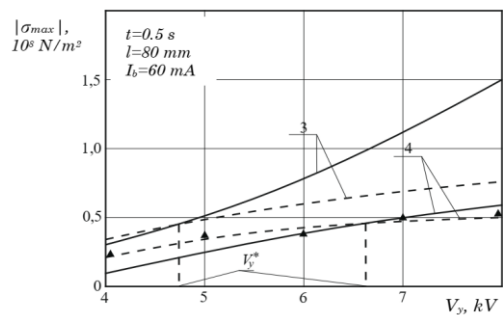


Fig. 4 – Dependence of the modulus of thermoelastic stresses $|\sigma_{\max}|$ on the upper side of a rectangular element on the time of exposure to the SEB: 1 – $I_b = 100$ mA, $V_y = 5$ kV, $l = 80$ mm, $V = 0,005$ m/s; 2 – $I_b = 60$ mA, $V_y = 7$ kV, $l = 80$ mm, $V = 0,005$ m/s; 3 – $I_b = 60$ mA, $V_y = 7$ kV, $l = 80$ mm, $V = 0,05$ m/s; 4 – $I_b = 100$ mA, $V_y = 5$ kV, $l = 80$ mm, $V = 0,05$ m/s

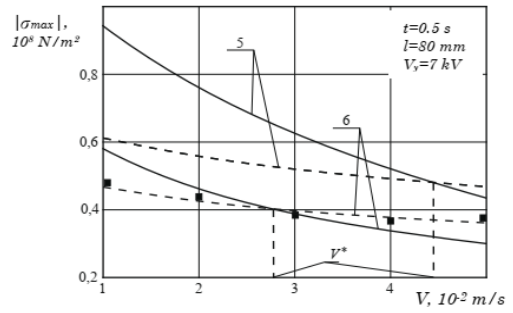
With variation of the SEB parameters, the magnitude of $|\sigma|$ may reach its limiting values σ^* (I_n^* , V_y^* , V^* , l^* , t^*) (I_n^* , V_y^* , V^* , l^* , t^* – SEB parameter values at which the condition $\sigma_{\max} = \sigma^*$ is satisfied), the exceedance of which leads to the destruction of the upper surface of the treated element. For all investigated ranges of SEB parameter variation, failure of the lower surface of the treated element does not occur. For treatment durations $t \geq 0,4...0,5$ s, a quasi-stationary thermal influence mode of the SEB on the rectangular element is observed, i.e., $|\sigma_{\max}|$ becomes independent of t .



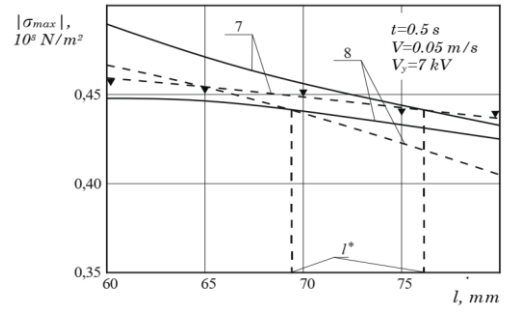
a)



b)



c)



d)

Fig. 5 – The influence of the SEP parameters on the value of the thermoelastic stress modulus $|\sigma_{\max}|$ on the upper side of the rectangular element: a) – the influence of the electron flow current I_b (1 – $V_y = 8$ kV, 2 – $V_y = 4$ kV; ● – experimental data for $V_y = 4$ kV [1, 6, 13-15]); b) – the influence of accelerating voltage V_y (3 – $V = 0,005$ m/s, 4 – $V = 0,05$ m/s; ▲ – experimental data for $V = 0,05$ m/s); c) – the influence of the speed of movement of the electron flow V (5 – $I_b = 60$ mA, 6 – $I_b = 50$ mA; ■ – experimental data for $I_b = 50$ mA); d) – influence of distance from the treated surface l (7 – $I_b = 70$ mA, 8 – $I_b = 50$ mA; ▼ – experimental data for $I_b = 70$ mA) (the rest of the notation is similar to Fig. 3)

Therefore, the influence of treatment time on the permissible SEB parameter values is observed for $0 < t < 0,4...0,5$ s, and is practically absent for $t \geq 0,4...0,5$ s. So, for example, for $0 < t \leq 0,015$ s, the permissible values of the SEB parameters are $50 \text{ mA} \leq I_n \leq 100 \text{ mA}$, $4 \text{ kV} \leq V_y \leq 5 \text{ kV}$, $l = 80 \text{ mm}$, $0,005 \text{ m/s} \leq V \leq 0,05 \text{ m/s}$; for $0 < t \leq 0,075$ s – $50 \text{ mA} \leq I_n \leq 100 \text{ mA}$, $4 \text{ kV} \leq V_y \leq 5 \text{ kV}$, $l = 80 \text{ mm}$, $V = 0,05 \text{ m/s}$; for $0 < t < 0,083$ s – $50 \text{ mA} \leq I_n \leq 60 \text{ mA}$, $4 \text{ kV} \leq V_y \leq 7 \text{ kV}$, $l = 80 \text{ mm}$, $V = 0,005 \text{ m/s}$; for $0 < t \leq 0,092$ s – $50 \text{ mA} \leq I_n \leq 60 \text{ mA}$, $4 \text{ kV} \leq V_y \leq 7 \text{ kV}$, $l = 80 \text{ mm}$, $V = 0,05 \text{ m/s}$.

At $t \geq 0.5$ s, the permissible ranges of changes in the SEP parameters become (Fig. 6): at $l = 80$ mm and $V = 0,05$ m/s – $75 \text{ mA} \leq I_b \leq 130 \text{ mA}$, $4 \text{ kV} \leq V_y \leq 8 \text{ kV}$; at $I_b = 60$ mA and $l = 80$ mm – $4,8 \text{ kV} \leq V_y \leq 6,9 \text{ kV}$, $0,005 \text{ m/s} \leq V \leq 0,05 \text{ m/s}$; at $V_y = 7$ kV and $l = 80$ mm – $50 \text{ mA} \leq I_n \leq 75 \text{ mA}$, $0,028 \text{ m/s} \leq V \leq 0,043 \text{ m/s}$; at $V_y = 7$ kV and $V = 0,05$ m/s – $50 \text{ mA} \leq I_n \leq 90 \text{ mA}$ and $68 \text{ mm} \leq l \leq 80 \text{ mm}$

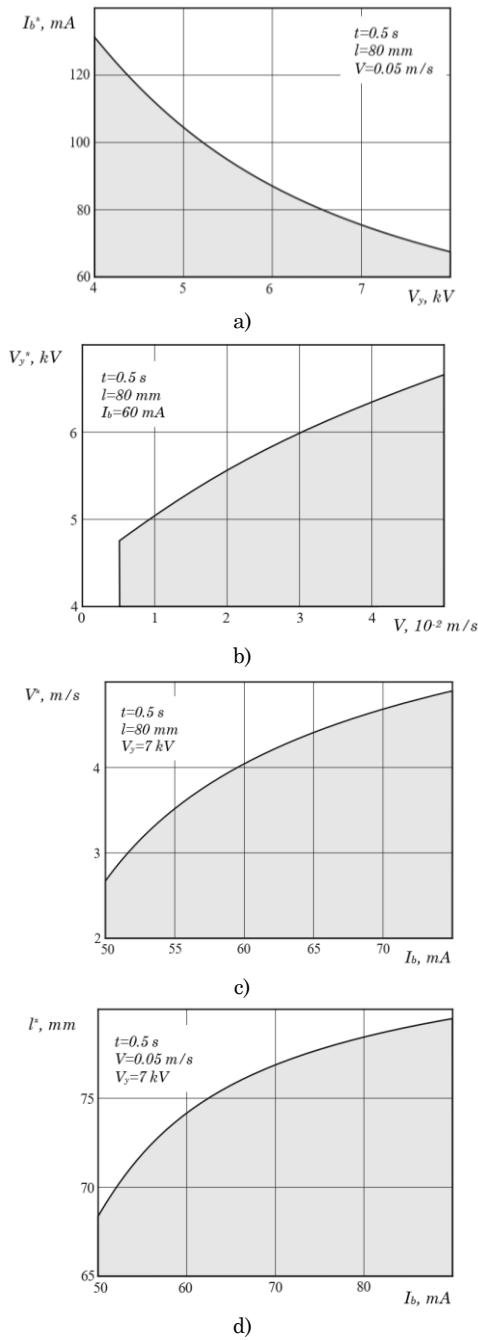


Fig. 6 – Areas of permissible values of SEB parameters during electronic processing of rectangular elements (shaded areas): a) – $60 \text{ mA} \leq I_n \leq 130 \text{ mA}$, $4 \text{ kV} \leq V_y \leq 8 \text{ kV}$; b) – $4,8 \text{ kV} \leq V_y \leq 6,9 \text{ kV}$, $0,005 \text{ m/s} \leq V \leq 0,05 \text{ m/s}$; c) – $50 \text{ mA} \leq I_n \leq 75 \text{ mA}$, $0,028 \text{ m/s} \leq V \leq 0,043 \text{ m/s}$; d) – $50 \text{ mA} \leq I_n \leq 90 \text{ mA}$, $68 \text{ mm} \leq l \leq 80 \text{ mm}$ (the rest of the notation is similar to Fig. 3)

Comparison of the calculation results with selected experimental data obtained in [10, 11, 13-15] (see Fig. 5) shows complete qualitative agreement, while the quantitative difference between them does not exceed 8-

10 %. In addition, the experimental data obtained from the development of technological processes for thermal strengthening of KO2 optical ceramics indicate that both at the initial stage (within tenths of a second) of optical ceramic processing and at later stages (ranging from several seconds to tens of seconds), surface destruction of the material (formation of cracks, chipping, and other defects) is observed under certain combinations of SEB parameters, which also corresponds to the obtained calculation results.

Thus, the developed mathematical models for calculating thermal stresses in the areas of maximum external thermal influence on the surface of a rectangular element (single-cycle SEB treatment) can, at the stages of developing technological processes for surface thermal strengthening of optical ceramics, predict (with a relative error of 8-10 %) the so-called “critical” or “dangerous” regimes – that is, combinations of SEB parameter values (I_n^* , V_y^* , V^* , l^* , t^*) exceeding their permissible limits, under which the treated material fails. This makes it possible to increase the efficiency of final surface treatment of optical components made of optical ceramics using SEB technology, with the aim of improving the mechanical strength of their surface layers, which ultimately enhances the reliability, safety, and stable operation of electrical power system components under extreme electrical and thermal loads.

3. CONCLUSIONS

1. Mathematical models have been developed to describe the thermal influence of a strip electron beam (SEB) on optical elements of rectangular shape. Unlike existing models, these take into account:

- the results of SEB probing, which relate its energy characteristics (heat flux density and exposure duration) to the controllable parameters of the electron-beam installation (beam current, accelerating voltage, distance to the treated surface, and SEB scanning speed);
- the temperature dependences of the thermophysical properties of the optical material (volumetric heat capacity and thermal conductivity coefficient), which makes it possible to more accurately calculate the temperature and thermomechanical stress distributions across the thickness of the optical element in the regions of maximum external SEB influence (the most “critical” surface areas) as functions of the controllable installation parameters.

2. The ranges of permissible variations of the controllable parameters of the electron-beam installation have been determined, exceeding which leads to the loss of integrity of the surface layers of the processed optical ceramics (KO2, KO4, etc.). This results in the formation of cracks and chips, as well as noticeable structural changes that significantly reduce the infrared transmission coefficient of the optical material (by more than 1.5-2 times) and, ultimately, lead to failures of power engineering system components.

REFERENCES

1. V.A. Vashchenko, I.V. Yatsenko, YU.H. Leha, O.V. Kyrychenko, *Osnovy elektronnoyi obrobky vyrobiv z optychnykh materialiv. Monografiya* (Kyiv: Naukova dumka: 2011) [In Ukrainian].
2. *Handbook of Optical Engineering* (Ed. by Daniel Malacara) (CRC Press: 2020).
3. Woohong Kim, Guillermo Villalobos, Colin Baker, *Appl. Opt.* **54** No 31, F210 (2015).
4. S.F. Wang, et al., *Progr. Solid State Chem.* **41** No 1-2, 20 (2013).
5. W. Kim et al., *NRL (Naval Research Laboratory) Review of Transparent Ceramics for High-Energy Optics* (2015).
6. V.A. Vashchenko, D. I. Kotelnikov, YU.G. Lega, D.M. Krasnov, I.V. Yatsenko, O.V. Kirichenko, *Teplovyye protsessy pri elektronnoy obrabotke opticheskikh materialov i ekspluatatsii izdeliy na ikh osnove. Monografiya* (Kyiv: Naukova dumka: 2006) [In Russian].
7. *Processing, Properties, and Applications of Glass and Optical Materials* (Ed. by Arun K. Varshneya, Helmut A. Schaeffer) (John Wiley and Sons, Inc.: Hoboken, New Jersey: 2012).
8. I.V. Yatsenko, S.V. Antonyuk, V.A. Vaschenko, V.V. Tsybulin, *J. Nano-Electron. Phys.* **8** No 1, 01027 (2016).
9. *Handbook of Optical Materials* (Ed. by Marvin J. Weber). (CRC Press, Boca Raton, Florida: 2003).
10. I.V. Yatsenko, S.V. Antonyuk, V.I. Gordienko, V.A. Vaschenko, *J. Nano-Electron. Phys.* **9** No 1, 01010 (2017).
11. I.V. Yatsenko, V.S. Antonyuk, V.I. Gordienko, O.V. Kiritchenko, V.A. Vaschenko, *J. Nano-Electron. Phys.* **10** No 4, 04028 (2018).
12. Andrei D. Polyinin, Alexander V. Manzhurov, *Handbook of Mathematics for Engineers and Scientists (Advances in Applied Mathematics), 1st Edition* (Chapman and Hall/CRC: 2006).
13. I.V. Yatsenko, V.S. Antonyuk, V.A. Vashchenko, O.V. Kyrychenko, O.M. Tishchenko, *J. Nano-Electron. Phys.* **11** No 2, 02014 (2019).
14. I.V. Yatsenko, V.S. Antonyuk, V.A. Vashchenko, V.I. Gordienko, S.O. Kolinko, T.I. Butenko, *J. Nano-Electron. Phys.* **14** No 4, 04012 (2022).
15. I.V. Yatsenko, V.S. Antonyuk, V.P. Maslov, V.A. Vashchenko, V.I. Gordienko, S.O. Kolinko, T.I. Butenko, *J. Nano-Electron. Phys.* **15** No 4, 05030 (2023).

Математичне моделювання допустимих термопружних напружень в оптичних елементах електроенергетичних систем

I.V. Яценко¹, В.С. Антонюк², В.А. Ващенко¹, Гордієнко В.І.¹, В.П. Маслов³, Т.І. Бутенко¹

¹ Черкаський державний технологічний університет, 18030 Черкаси, Україна

² Національний технічний університет України «КПІ ім. Ігоря Сікорського», 03056 Київ, Україна

³ Інститут фізики напівпровідників ім. В.Є. Лашкарьова НАН України, 02000 Київ, Україна

Розроблено математичні моделі теплового впливу стрічкового електронного потоку на оптичні елементи, що враховують результати його зондування, геометричну форму та розміри елементів, а також температурні залежності теплофізичних властивостей оптичного матеріалу (об'ємної теплоємності, коефіцієнта теплопровідності), що дозволяє більш точно розраховувати розподіли температури та термопружних напружень по товщині оптичного елемента в зонах максимального зовнішнього впливу стрічкового електронного потоку (СЕП). Запропоновані моделі дозволяють точніше розрахувати вплив керованих параметрів електронно-променевої установки (струму променя, прискорювальної напруги, відстані до оброблюваної поверхні та швидкості переміщення СЕП) на розподіл термопружних напружень по товщині елементів та визначити допустимі діапазони їх зміни, перевищення яких призводить до руйнування елементів та відмови виробів електроенергетичних систем на їх основі. Це дозволяє підвищити ефективність фінішної поверхневої обробки за допомогою СЕП оптичних виробів з оптичних керамік з метою збільшення механічної міцності їх поверхневих шарів, що призводить, у остаточному підсумку, до підвищення надійності, безпечності та стабільної роботи виробів електроенергетичних систем в умовах екстремальних електричних та термічних навантажень.

Ключові слова: Математичні моделі, Електроенергетична система, Електронно-променева технологія, Оптична кераміка, Методи теорії теплопровідності та термопружності.